VERTICAL MICRO-NANOCHANNEL INTEGRATION FOR RELATIVE SURFACE PROTEIN ABUNDANCE QUANTIFICATION ON LIPOSARCOMA EXTRACELLULAR VESICLES

Premanshu K. Singh[1], Ali F. Usmani[1], Patricia Sarchet[1], Raphael Pollock[1] and Shaurya Prakash[1]*
[1]The Ohio State University, Columbus, Ohio, USA

ABSTRACT

We report on a vertically integrated micro-nanofluidic device for isolating and characterizing liposarcoma extracellular vesicles (EVs). Our device integrates microfiltration and immunoaffinity-based EV capture on the same device, yielding efficient isolation as demonstrated using cancer cell-conditioned media. Surface protein analysis of the extracellular vesicles showed differences in the two well-known surface tetraspanin molecules, CD63 and CD81. The isolation with anti-CD81 capture antibodies yielded higher EV-associated DNA than the anti-CD63 antibodies. To our knowledge, this is the first report on differences in surface protein expression that were exploited to capture cancer-relevant extracellular vesicles for sarcoma. Further analysis showed total DNA extraction capability compared to existing state of art methods with a significantly reduced processing time of approximately 85%. This innovation enhances EV-based liquid biopsy diagnostics.

KEYWORDS

Liposarcoma, *MDM2* DNA, Point-of-care diagnostics, Extracellular vesicles, and surface proteins.

INTRODUCTION

Soft tissue sarcomas (STS) are tumors originating from mesenchymal tissues and can develop in various anatomical sites throughout the body [1]. Among over 100 different sub-types of STS, liposarcoma (LPS) comprises up to 20% of all malignant cases and shows a median survival rate of < 1 year [2]. Further classification of LPS based on histology and biological factors includes well-differentiated (WDLPS), de-differentiated (DDLPS), myxoid, and pleomorphic, among which WDLPS and DDLPS are most prevalent [2,3]. Surgery remains the primary therapeutic approach for LPS. However, despite the addition of adjuvant treatments, over 50% of patients still develop recurrent or metastatic disease [4]. LPS is a lethal cancer for which we lack the means to unequivocally detect recurrence early when a cure may still be possible *via* adjuvant therapeutic interventions. Early detection of LPS recurrence is challenging as radiologic scans lack specificity, necessitating image-directed or open tissue biopsy resulting in time delays, significant costs, and patient discomfort [2,4]. Alternatively, a liquid biopsy is minimally invasive but requires a specific and reliable biomarker. WD/DDLPS both have amplified 12q13-15 locus on chromosome 12, which contains *MDM2*, the most commonly over-expressed LPS gene [5]. WDLPS contains mutated p53, whereas DDLPS consistently has wild-type (wt) p53. Both over-express *MDM2* DNA, leading to *MDM2* protein over-production that may override p53 tumor suppression, thereby serving as a key LPS driver; the underlying mechanisms remain uncertain [5].

In the quest to find a reliable biomarker for LPS recurrence, extracellular vesicles (EVs) have found a key niche [6]. EVs are 30-1000 nm lipid bilayer membrane-enclosed nanoparticles that are secreted by nearly all cells. EVs carry a diverse cargo, including DNA, RNA, and proteins, shielded from enzymatic destruction by the lipid bilayer, making them highly intriguing entities for biomarker analysis [7]. It has been shown that LPS EVs are shed into the peripheral blood and have high levels of *MDM2* DNA that are elevated versus normal control EVs or peri-tumoral normal tissues [8]. The critical technical challenge lies in isolating EVs with adequate purity and yield from a complex biofluid matrix to yield enough DNA for reliable diagnostic value, applicable within clinical settings. Past reports suggest that ~10^{10} EVs/10^6 cells (approximately equivalent to 5 ng/µL of total DNA) are required for performing viable assays [7].

At present, the effective isolation of EVs and their cargo in substantial quantities and high purity remains a significant challenge. The isolation of EVs through accepted methods, such as ultracentrifugation (UC), size exclusion chromatography, and polymer-based precipitation techniques, presents challenges due to their labor-intensive nature and the need for specialized laboratory equipment [7]. Consequently, microfluidic technologies, targeting key EV features like size, shape, electric charge, electric polarizability, and surface proteins as critical parameters for separation-based techniques have seen drastic growth recently [9]. However, current microfluidic devices encounter challenges in their utilization stemming from intricate designs and fabrication procedures, inadequate quality of captured EVs, reduced purity in extracting EV cargo, or the concurrent isolation of multiple EV subtypes [7].

The challenges in the diagnosis and prognosis of LPS, coupled with the importance of EV *MDM2* DNA as a biomarker and the limitations of UC in retrieving EVs and EV cargo, motivated us to explore innovative "chip-based" technologies using microfluidics. Our proof-of-concept device (Figure 1) is a multi-layer microfluidic device with a nanofluidic interconnect to isolate, capture, and elute EVs from liposarcoma cell conditioned media (LCCM) with a clear advantage over existing methods for LPS-relevant EV-cargo extracted from the biofluid. Our microfluidic device combines two essential unit operations, namely size-based isolation via microfiltration and immunoaffinity-based capture of extracellular vesicles (EVs), sequentially. This integration facilitates the design, fabrication, and operation of the device, offering significant advantages over previous microfluidic approaches.

The EV capture efficacy of our device relies on the judicious selection of surface proteins on EVs for immunocapture. There are no in-depth reports on the surface protein distribution for LPS-derived EVs. The group of tetraspanin proteins including CD9, CD63, CD37, CD81, and/or CD82 are some of the most common specific markers of endosome-derived EVs (such as small EVs or sEVs with average size < 200 nm) [10]. Several studies describe CD63 and CD81 as the most frequently identified proteins in sEVs and are considered their classical markers [11]. In fact, in many cells, the bulk of CD63 has been described as typical in intracellular compartments of endosome/lysosomal origin [11]. Past reports show that these tetraspanins are unevenly distributed across the EVs, with the tetraspanin profile being consistent within a given EV source regardless of isolation method, but different across various sources [12]. EV tetraspanin profiles are also shown to be disease-specific [12]. For instance, in a study by Okada et al., heterogeneous expression levels and distributions of 3 major tetraspanins (CD9, CD63, and CD81) were reported for sEVs in serum, plasma, CSF, and brain samples [13]. Moreover, the heterogeneous distributions and predominant tetraspanins were specific to each biofluid [13]. In

978-1-940470-05-4/HH2024/$25©2024TRF
DOI 10.31438/TRF.HH2024.89

this work, we evaluate the heterogeneity of surface tetraspanin expressions on LPS-derived EVs, specifically, our report analyzes the specificity of EV capture for multiple tetraspanin proteins, for two molecules - CD63 and CD81, aiding in selecting the best antibody target for maximum EV capture towards the long-term goal of improving EV yields and purity.

MATERIALS AND METHODS

Cell Culture

Previously established human LPS cell line Lipo246 [14] was used for EV production. Briefly, Lipo246 cells were grown in Dulbecco's Modified Eagle Medium (DMEM; Gibco) and supplemented with 10% (vol/vol) Fetal Bovine Serum (FBS). Afterwards, the cells were serum-starved with serum-free DMEM for 48 h for EV production and Lipo246 cell line conditioned media (LCCM) was subsequently collected. LCCM was centrifuged (Eppendorf Centrifuge 5810 R) at 2000 g and 4°C for 20 min and stored at -80°C.

Device Fabrication

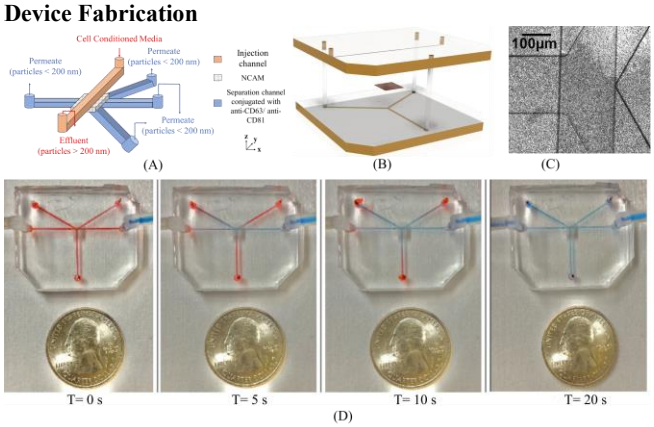

Figure 1: Device layout. (A) Schematic of the microfluidic device, depicting the inlet and the EV-capturing antibody functionalized microchannels vertically integrated to inlet microchannel through 200 nm nanochannels in the nanocapillary array membranes (NCAMs). The flow path is also shown. (B) 3D-rendering of the device layers (microchannel inlet: 3 cm (L) x 500 µm (W) x 60 µm (H)), 3-outlet separation channels (each (1.5 cm (L) x 500 µm (W) x 60 µm(H)). (C) Optical micrograph of the device showing inlet-outlet channel interface. Scale= 100 µm. (D) A time-lapse image showing incoming flow (blue-dye) exiting through outlet (separation channels) after going through the nanocapillaries. Initially, channels were filled with red-dye for flow visualization.

Our device consists of an injection microchannel (3 cm x 500 µm x 60 µm) which acts as the sample inlet path and is vertically integrated through 200 nm nanocapillaries (5 x 5 mm²) to a bottom layer with three separation microchannels (1.5 cm x 500 µm x 60 µm each) functionalized with capture antibodies for EV immunocapture. The vertically integrated micro-nanofluidic device was fabricated using polydimethylsiloxane (PDMS) using soft lithography. The microchannel features were first patterned on an n-type 4" silicon wafer using standard UV lithography to generate a negative mold for casting PDMS. Briefly, the silicon wafer was cleaned with a piranha (H_2SO_4:H_2O_2 (3:1)) solution for 10 minutes, rinsed with de-ionized water, dried with nitrogen, and baked at 200°C for 15 mins. Post dehydration bake, the silicon wafer was spin-coated with SU-8 2050 at 2500 rpm for 40 s, and soft baked at 65°C for 3 mins and at 95°C for 8 mins. The soft-baked wafer was exposed to 10 mW/cm^2 UV light for 17.5 s using a UV contact aligner (EV Group 620 contact aligner; wavelength: 365 nm), followed by a post-exposure bake at 65°C for 2 mins and at 95°C for 6 mins. The exposed pattern was then developed in SU-8 developer for 6 mins and hard baked at 200°C for 30 mins.

The silicone elastomer base and curing agent (from Ellsworth Adhesives) were combined at a 10:1 ratio, then poured onto the silicon master, degassed, and cured at 70°C for 4 hours. The cured PDMS was peeled off the silicon master and cut into individual channels. Through-holes were punched with 1.5 mm biopsy punches on the PDMS with the injection channel to access the injection channel and the separation channel. A nanocapillary array membrane (NCAM; GE Water & Process Technologies), featuring a nominal capillary diameter of 200 nm, served as the nanofluidic separator. The 5 mm x 5 mm NCAM underwent silanization in a nitrogen glove bag with a 3% v/v (3-Aminopropyl) triethoxysilane (APTES; Sigma Aldrich) solution in anhydrous ethanol for 1.5 minutes. Subsequently, both the silanized NCAM and the PDMS monolith with the injection channel were subjected to oxygen plasma treatment at 600 mTorr for 15 seconds and bonded together, aligning the NCAM over the middle of the injection channel along its length through visual inspection. Finally, the PDMS containing the monolith of the separation channel and the NCAM-injection channel underwent another round of oxygen plasma treatment at 600 mTorr for 15 seconds. The treated surfaces were then bonded with their channels aligned perpendicular through visual inspection.

Surface Modification for EV Immunocapture

The separation channel was plasma activated and treated with APTES solution (2% v/v) in anhydrous ethanol (Decon Labs Inc.) 20 µL APTES solution was flushed in the channel 5 times at 3 min intervals, and incubated for 2 h [7]. After 2 hours, 20 µL of anhydrous ethanol was flushed through the separation channel to remove any physiosorbed APTES. Next, the separation channel was flushed with 1.25% glutaraldehyde solution in 1X phosphate buffer saline (PBS; Corning) every 3 minutes for 15 minutes and left to incubate for 30 minutes at 4°C. Following the incubation, the channel was flushed with 1X PBS three times to remove any physiosorbed glutaraldehyde molecules. Finally, 50 µg/mL of primary antibody anti-CD63 or anti-CD81 (Ancell) diluted in 1X PBS was flushed through the separation channel and left to incubate at 4°C for 8 hours. The separation channel was flushed with 1X PBS after the incubation to remove any physiosorbed antibody with the device stored at 4°C until further use [7].

EV Capture and Elution

A falcon tube containing LCCM was removed from the -80°C refrigerator and thawed at 4°C. The microfluidic device was perfused with LCCM at 10 µL/min for 45 min using a syringe pump (Harvard Apparatus) with the LCCM-containing syringe connected to the inlet of the injection channel *via* a tubing (0.8 mm inner diameter; US Plastic) using barbed nylon connectors (Cole-Parmer).

After the experiment, the separation channel was flushed five times with 1X PBS to rinse the channel and remove any loosely bound EVs. Next, the captured EVs in the separation channel were eluted by flushing 60 µL of pH 2.2 glycine-HCl buffer [7], and the 60 µL of elution fluid was collected in an Eppendorf tube. Next, 120 µL of Tris-HCl buffer was added to the eluted solution to neutralize the pH of the glycine-HCl buffer containing the EVs to ~ pH 7.4. Finally, the captured EV solution was stored at -80°C until further use.

Verification of EV Capture and Release

LCCM microfiltered with a 220 nm PVDF syringe filter (Restek Technologies) was perfused at a flow rate of 0.5 µL/min

through a separation channel plasma bonded to a #1.5 thickness coverslip. This flow rate was selected to replicate the flow conditions observed in the separation channel of our device when the injection channel is perfused at a flow rate of 10 µL/min [7]. DiO dye (ThermoFisher Scientific) was used to fluorescently tag the captured EVs. 20 µL of 1 µM DiO dye in 1X PBS was flushed through the separation channel and incubated at room temperature for 10 minutes following the LCCM perfusion. Confocal microscopy (Olympus FV3000) confirmed the presence of captured EVs in the separation channel, indicated by increased fluorescence post-tagging captured EVs with DiO dye (Figures 2B and 2E). After elution of the captured EVs with a glycine-HCl buffer, the fluorescence decreased, indicating the successful release of captured EVs (Figures 2C and 2F).

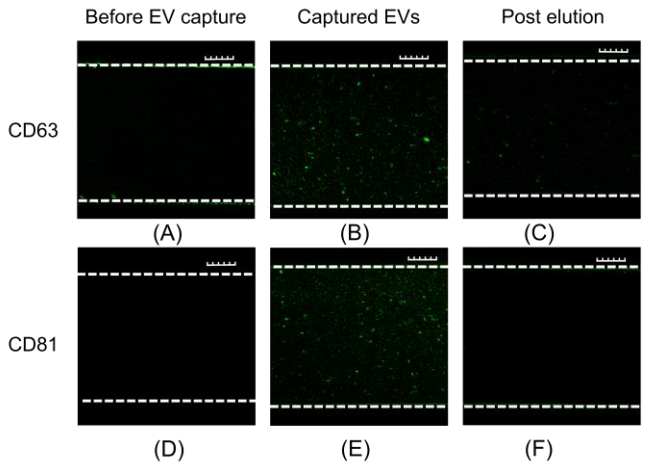

Figure 2: EV capture validation. Fluorescence verification for capture and elution of EVs for different combinations of antibodies. A, D, and G (before fluorescently tagging the captured EVs in the separation channel) showed no significant fluorescence (no green). The fluorescence signal (green) increased significantly in B, E, and H (post-tagging the capture EVs with DiO dye). A decrease in fluorescence signal was observed in C, F, and I (following elution with pH 2.2 glycine-HCl buffer). Scale bar = 100 µm.

Transmission Electron Microscopy

The EVs isolated from the device were observed using transmission electron microscopy (TEM), post-fixation, and staining. 7.5 µL of isolated EVs solution was placed on a glow discharged formvar coated and carbon stabilized copper grid (Electron Microscopy Sciences, Hartfield, PA) at room temperature. After 20 mins, the TEM grid was washed twice with phosphate buffer (pH = 7.4) and fixed with 7.5 µL of 1.25% glutaraldehyde for 5 mins at room temperature. Post the fixation step, the grid was rinsed with DI water three times and immediately stained with 1% (w/v) uranyl-acetate in double distilled H_2O (ddH_2O) for 15 s. The grid was then air-dried after manually removing any excess liquid with blotting paper. Transmission electron microscopy images were obtained using a FEI Tecnai G2 Spirit microscope (80 kV accelerating potential), at The Ohio State University Campus Microscopy & Imaging Facility (CMIF). ImageJ (v1.44) was used to post-process the micrographs.

DNA Quantification and Real-Time PCR of *MDM2* DNA

EV samples isolated, captured, and eluted from four devices were pooled to ensure an adequate sample volume for subsequent DNA. DNA extraction from this pooled sample was performed using the QIAGEN QIAamp DNA kit following the instruction manual provided by the kit manufacturer. The final elution of the precipitated and washed DNA from the column was done using 100 µL of double-distilled H_2O, followed by vacuum spinning for 1 hour and 15 minutes to increase the DNA concentration of the sample and remove debris and contaminants [8]. The dried sample was re-suspended in 16 µL of double-distilled H2O and vortexed thoroughly for proper mixing. Subsequently, 1 µL of this sample was used for DNA quantification, and the remaining 15 µL was utilized for PCR analysis. The expression level of *MDM2* of the isolated EVs was determined using DNA sequence-specific probes (*MDM2*- Hs00540450_s1, Thermo Fisher). All samples were measured in triplicates.

RESULTS AND DISCUSSION

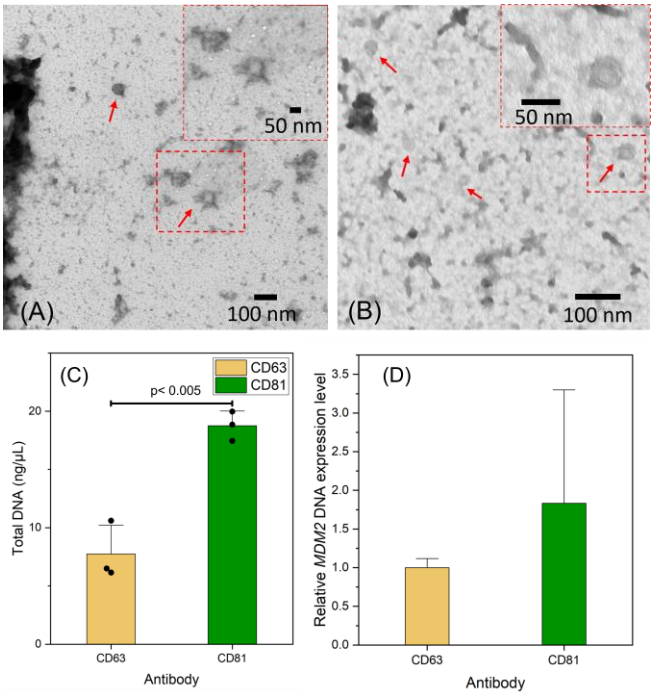

Figure 3: EV analysis. (A), (B) Electron-dense particles (red arrows) with cup-shaped morphology imaged using TEM microscopy confirmed the presence of EVs in the isolated sample. Close-up images of EVs are included at the top right corner. EVs captured show a difference in total DNA content (C) and MDM2 DNA expression level (D) depending on the choice of tetraspanin molecule used to capture the EVs. Each data point contains pooled fluid contributing a total of ~180 µL of EV-enriched fluid per test. Grubbs' test for outliers was used for the outlier detection in the data. Data is represented as mean ± SD.

Negative stain transmission electron microscopy (TEM) was employed to morphologically characterize the isolated EV samples. The TEM micrographs revealed a diverse array of EVs in terms of size, shape, and density. A representative image set is shown in Figure 3A and Figure 3B with the characteristic cup-shaped morphology [15,16] for EVs used to visually confirm the presence of EVs.

The use of CD81 as a target tetraspanin for the capture of EVs resulted in a significantly higher ($p < 0.005$) total DNA yield from the isolated EV samples (Figure 3C). The total DNA extracted from the CD81 surface functionalized devices was observed to be ~2x higher than the devices functionalized with CD63 antibodies.

The time taken for the EV isolation and preparation for analysis

was recorded. Our device yielded comparable total DNA yield to gold-standard EV isolation techniques like Ultracentrifugation (UC). Notably, our device achieved this efficiency using only 450 uL of LCCM perfused through the injection channel over a 45-minute isolation period, contrasting with UC which requires 15 mL of LCCM and 4 hours for isolation [7].

Past work from our team has shown that *MDM2* DNA upregulation in patient-derived tissue and blood EVs (30-200 nm lipid-based nanoparticles) is directly correlated to the recurrence of LPS tumors [8,17]. Therefore, it is crucial to ensure that the isolation process does not compromise the integrity of *MDM2* DNA. RT-PCR analysis of the isolated EV samples for *MDM2* DNA confirmed its presence, indicating that the EVs subjected to the isolation, capture, and elution process in the device maintain the integrity of their internal cargo. Preliminary findings on the relative expression levels of *MDM2* DNA in isolated EVs suggest a higher expression in EVs isolated using anti-CD81 antibodies, as illustrated in Figure 3D.

CONCLUSION

We report on isolating liposarcoma (LPS) EVs in an innovative multi-layer, vertically integrated micro-nanofluidic device. This is the first report on the relative surface protein abundance quantification on LPS EVs. Our study revealed different expression of surface proteins CD63 and CD81 on LPS EVs, with the use of CD81 tetraspanin for EV capture resulting in a two-fold increase in total DNA extraction compared to CD63. This finding aids in optimizing our device for enhanced EV isolation and DNA extraction. Additionally, our device demonstrated a remarkable capability, extracting comparable amounts of total DNA from EVs compared to UC which is considered a gold standard technique for EV isolation. Moreover, our device significantly reduces processing time, by approximately 85% compared to UC, offering potential for point-of-care diagnostics.

ACKNOWLEDGEMENTS

The authors would like to acknowledge the resources from the Campus Microscopy and Imaging Facility (CMIF) and the OSUCCC Microscopy Shared Resource (MSR) at The Ohio State University. This work was supported by the US Department of Defense through the Peer Reviewed Cancer Research Program under Grant CA210874.

REFERENCES

[1] A.C. Gamboa, A. Gronchi, K. Cardona, "Soft-tissue sarcoma in adults: An update on the current state of histiotype-specific management in an era of personalized medicine", *CA: A Cancer Journal for Clinicians*, 70, 200-229 (2020).

[2] V. Karavasilis, B.M. Seddon, S. Ashley, O. Al-Muderis, C. Fisher, I. Judson, "Significant clinical benefit of first-line palliative chemotherapy in advanced soft-tissue sarcoma - Retrospective analysis and identification of prognostic factors in 488 patients", *Cancer*, 112, 1585-1591 (2008).

[3] K. Thway, "Pathology of Soft Tissue Sarcomas", *Clinical Oncology*, 21, 695-705 (2009).

[4] M. C. Tan, M.F. Brennan, D. Kuk, N.P. Agaram, C.R. Antonescu, L.X. Qin, N. Moraco, A.M. Crago, and S. Singer, "Histology-based Classification Predicts Pattern of Recurrence and Improves Risk Stratification in Primary Retroperitoneal Sarcoma", *Annals of surgery,* 263, 593-600 (2016).

[5] A. Laroche-Clary, V. Chaire, M.P. Algeo, M.A. Derieppe, F.L. Loarer, and A. Italiano, "Combined targeting of MDM2 and CDK4 is synergistic in dedifferentiated liposarcomas", *Journal of Hematology & Oncology*, 10, 123 (2017).

[6] G. van Niel, G. D'Angelo, G. Raposo, "Shedding light on the cell biology of extracellular vesicles", *Nature Reviews Molecular Cell Biology*, 19, 213-228 (2018).

[7] L. Casadei, A. Choudhury, P. Sarchet, P. M. Sundaram,G. Lopez, D. Braggio, G. Balakirsky, R. Pollock, and S. Prakash, "Cross-flow microfiltration for isolation, selective capture and release of liposarcoma extracellular vesicles", *Journal of Extracellular Vesicles*, 10(4), e12062 (2021).

[8] L. Casadei, F. Calore, D.A. Braggio, A. Zewdu, A.A. Deshmukh, P. Fadda, G. Lopez, M. Wabitsch, C. Song, J.L. Leight, V.P. Grignol, D. Lev, C.M. Croce, and R.E. Pollock, "MDM2 Derived from Dedifferentiated Liposarcoma Extracellular Vesicles Induces MMP2 Production from Preadipocytes", *Cancer Research*, 79, 4911-4922 (2019).

[9] P.K. Singh, A. Patel, A. Kaffenes, C. Hord, D. Kesterson, and S. Prakash, "Microfluidic Approaches and Methods Enabling Extracellular Vesicle Isolation for Cancer Diagnostics", *Micromachines*, 13(1),139 (2022).

[10] E. Willms, C. Cabañas, I. Mäger, M.J.A. Wood, P. Vader, "Extracellular Vesicle Heterogeneity: Subpopulations, Isolation Techniques, and Diverse Functions in Cancer Progression", *Frontiers in Immunology*, 9, 738 (2018).

[11] Z. Andreu, M. Yáñez-Mó, "Tetraspanins in extracellular vesicle formation and function", *Frontiers in Immunology*, 5, 442 (2014).

[12] R. R. Mizenko, T. Brostoff, T. Rojalin, H.J. Koster, H.S. Swindell, G.S. Leiserowitz, A. Wang, and R.P. Carney, "Tetraspanins are unevenly distributed across single extracellular vesicles and bias sensitivity to multiplexed cancer biomarkers", *Journal of Nanobiotechnology*, 19, 250 (2021).

[13] M. Okada-Tsuchioka, N. Kajitani, W. Omori, T. Kurashige, S. Boku, and M. Takebayashi, "Tetraspanin heterogeneity of small extracellular vesicles in human biofluids and brain tissue", *Biochemical and Biophysical Research Communications*, 627, 146-151 (2022).

[14] T. Peng, P. Zhang, J. Liu, T. Nguyen, S. Bolshakov, R. Belousov, E.D. Young, X. Wang, K. Brewer, D.H. López-Terrada, A.M. Oliveira, A.J. Lazar and D. Lev, "An experimental model for the study of well-differentiated and dedifferentiated liposarcoma; deregulation of targetable tyrosine kinase receptors", *Laboratory Investigation*, 91, 392-403 (2011).

[15] K. Broad, S.A. Walker, I. Davidovich, K. Witwer, Y. Talmon, and J. Wolfram, "Unraveling multilayered extracellular vesicles: Speculation on cause", *Journal of Extracellular Vesicles*, 12, e12309 (2023).

[16] L. G. Rikkert, R. Nieuwland, L. Terstappen, F.A.W. Coumans, "Quality of extracellular vesicle images by transmission electron microscopy is operator and protocol dependent", *Journal of Extracellular Vesicles*, 8, 1555419 (2019).

[17] L. Casadei, P. Sarchet, F.C.C. de Faria, F. Calore, G. Nigita, S. Tahara, L. Cascione, M. Wabitsch, F.J. Hornicek, V. Grignol, C.M. Croce, and R.E. Pollock, "In situ hybridization to detect DNA amplification in extracellular vesicles", *Journal of Extracellular Vesicles*, 11(9), e12251 (2022).

CONTACT

*S. Prakash, tel: +1-614-6884045; prakash.31@osu.edu